Available online at www.CivileJournal.org

Civil Engineering Journal

(E-ISSN: 2476-3055; ISSN: 2676-6957)

Vol. 9, No. 11, November, 2023

Enhancing Environmental Sustainability in a Critical Region: Climate Change Impacts on Agriculture and Tourism

Kazem Javan [1*], Mehrdad Mirabi [2], Sajad Ahmad Hamidi [3], Mariam Darestani [4], Ali Altaee [1], John Zhou [1]

[1] *School of Civil and Environment, University of Technology Sydney, Sydney, Australia.*

[2] *Department of Civil and Environment, Ferdowsi University, Expert of Mashhad Water and Wastewater, Mashhad, Iran.*

[3] *Department of Physics and Engineering, Slippery Rock University of Pennsylvania, PA, United States.*

[4] *Department of Civil and Environment, Western Sydney University, Sydney, Australia.*

Received 18 May 2023; Revised 16 October 2023; Accepted 23 October 2023; Published 01 November 2023

Abstract

The Ardabil Plain is pivotal in the national agricultural sector and ranks among the leading agricultural and horticultural production provinces. The primary objective of this study is to enhance environmental sustainability in this critical and vulnerable region, particularly in the face of imminent droughts and climate change. The study examines the impacts of climate change on agriculture and tourism in the area. It puts forward suggestions for implementing sustainable practices to safeguard the well-being of the local population. The results indicate a 38% reduction in precipitation, especially in the autumn season, with a possible alteration in the timing and strength of rainfall. Also, a notable decline in production volume, particularly in a specific region of the Ardabil plain, has been observed. The Ardabil Plain currently produces 284,182 tons of wheat, with 204,980 tons from irrigated crops and 79,202 tons from rain-fed crops. However, the projected future scenario indicates a decrease in total wheat production to 209,196 tons, with 160,125 tons from irrigated crops and 49,071 tons from rain-fed crops. This decline in production is expected to lead to a total net income loss of approximately -$75,389,059, with -$45,095,663 attributed to irrigated crops and -$30,293,396 to rain-fed crops. The study findings suggest that the availability of water sources in certain regions may prompt a shift in farming land from the north to the south of the plain to promote environmental sustainability. This demographic change could have significant financial and social implications for the region's growth and prosperity. Moreover, increasing temperatures in the western and northern regions pose flood risks and uncomfortable travel conditions, particularly concerning given the reliance on tourism and potential unemployment consequences. It becomes imperative to adopt sustainable practices and manage resources effectively to ensure the region's resilience and prosperity in the face of environmental challenges.

Keywords: Environmental Sustainability; Climate Change Impacts; Agriculture; Financial Implications; Vulnerability; Ardabil Plain.

1. Introduction

Drought, a recurring phenomenon, has significant implications for agriculture, tourism, and other aspects in Iran, presenting a challenging reality that can hinder planning and prospects [1]. Climate change and rising temperatures contribute to the development of droughts, exacerbating their severity and frequency. Climate change has led to more frequent and severe droughts in arid and semi-arid regions, reducing water availability for various purposes. In a study conducted by Ozturk et al. as part of the Coordinated Regional Climate Downscaling Experiment, the influence of climate change on seasonal variations in precipitation and temperature was examined in a portion of Asia. The findings revealed a significant warming trend in surface temperatures in the south-eastern Pacific [2].

* Corresponding author: kazem.javan@student.uts.edu.au

http://dx.doi.org/10.28991/CEJ-2023-09-11-01

Iran is one of the countries that have experienced severe rainfall, floods, droughts, and extreme temperatures in recent years due to climate change [3, 4]. Ardabil province, one of the important geopolitical provinces of Iran, which plays an important role in the country's agriculture and tourism industries, has faced the problem of drought in recent decades [5]. Numerous research studies have been conducted in the Ardabil region, focusing on climate change and drought. Yazdani et al. (2021) utilized climate models to predict increasing precipitation in some months, such as March, January, and November, while observing a decrease in other months, which can have implications for water resources and drought patterns [5]. Similarly, Ghorbani et al. (2021) noted that temperature variations were more pronounced than precipitation changes in Ardabil, underlining the significance of rising temperatures in the region [6].

The agricultural industry in Ardabil province provides jobs for around a third of its residents [7–9]. Disruptions to agriculture caused by climate change can have severe economic consequences, impacting not only local farmers but also the country's overall agricultural output and food security. Fatahi et al. (2022) assessed climate suitability for sunflower cultivation in Ardabil, highlighting the importance of temperature and water availability for successful cultivation [10]. Ghanbari et al. (2021) analyzed climate parameters for corn cultivation and zoning in Ardabil, emphasizing the significance of temperature, rainfall, and topography [11]. Deihimfard et al. (2022) projected potential changes in water footprint for wheat agro-ecosystems in Iran, suggesting both positive and negative effects on water use efficiency due to climate change [12]. Satari & Khalilian (2020) explored the impact of climate change on soybean yield in Ardabil, Golestan, and Mazandaran provinces, forecasting increased yields in response to climate change [13]. Tayyebi et al. (2023) conducted a study to examine the uncertainties in estimating agricultural water demands over three future timeframes in the northern region of Ardabil province. This assessment involved 10 GCM models and 2 AR6 propagation scenarios. Additionally, they evaluated a total of nine adoption scenarios using the WEAP model, taking into account the available options [14].

In addition, the tourism industry, particularly water tourism, is another important sector that plays a role in the region's economy. Numerous hot springs and majestic snow-capped peaks attract tourists and generate revenue for the local community, which is a significant source of income and employment in Ardabil [15]. Research within the field of the tourism industry has been conducted in this region. Roshan et al. (2016) conducted a study to assess the impact of climate change on the Tourism Climate Index (TCI) in Iran. The research involved the calculation of monthly TCI values for 40 cities across Iran for the years spanning from 1961 to 2010. Subsequently, the study examined how the TCI changed over this period for each of the cities. The results showed that there were increases in TCI for at least one station every month, with some months showing no decreases. Notably, in October, a maximum of 45% of the stations exhibited significant changes in TCI, whereas in December, only 10% of stations demonstrated such changes [16]. Sobhani & Safarian (2020) used the TCI to evaluate climate comfort for tourism in northwestern Iran, providing insights into the seasonal suitability for tourism activities [17]. Amininia et al. (2020) focused on climate comfort in Ardabil province for health tourism, emphasizing its significance for attracting tourists [18].

The Ardabil Plain, in particular, holds great importance within this economic framework in Ardabil province. As both the agricultural and water tourism sectors heavily rely on water resources, extensive research has been conducted to address this crucial issue [19–21]. However, the region is also affected by drought-related issues and a general trend towards aridification, which poses challenges for agricultural activities [22, 23]. In the Ardabil Plain, previous studies have addressed climate change, as will be highlighted in this study. Nourani et al. (2023) examined the enduring effects of climate change on groundwater fluctuations within Iran's Ardabil Plain. To achieve this, they introduced a groundwater-level modeling approach. This involved utilizing climate change data derived from the outputs of Global Climate Models (GCMs) from the sixth report of the Coupled Model Intercomparison Project (CMIP6), as well as future scenario information from the Shared Socioeconomic Pathway 5-8.5. These climate change variables were integrated into machine learning models for analysis [24]. Nouri-Khajebelagh et al. (2022) conducted a study in Ardabil Plain, Iran, with the objective of assessing the overall value of water resources. They conducted separate valuations for agricultural water and drinking water. For agriculture, they used the production function method to evaluate major crops. Additionally, the study explored the willingness of individuals to pay extra for municipal drinking water. Ultimately, the findings from both the assessment of irrigation water and drinking water were integrated to determine the comprehensive value of water in the region [25].

There are numerous tools available for conducting research in the field of climate change, and one of these tools is Artificial Neural Networks (ANN). The application of ANN in climate change and water resource management has proven to be valuable in addressing complex challenges and improving decision-making processes. ANN models have been widely used to analyze and predict water-related phenomena, such as stream flow, groundwater levels, rainfall patterns, and water quality [26–28]. By training ANN models with historical data, they can learn and recognize patterns, relationships, and nonlinear dependencies within the data [29–31]. By analyzing real-time data inputs, including rainfall, river flow, and water levels, ANNs can help in predicting extreme events and issuing timely warnings, enabling proactive measures to mitigate potential damages, and utilizing Geographic Information Systems (GIS) to enhance water resource monitoring and mapping [32]. This integration allows for the efficient analysis of large-scale data sets, providing spatially distributed information on water availability, land use changes, and hydrological processes [33–35].

The Standardized Precipitation Index (SPI) is a useful tool for monitoring drought conditions and implementing early warning systems. It is calculated by standardizing observed precipitation data using long-term averages and standard deviations [36–38]. It has been widely adopted as a drought index due to its robustness, versatility, and ability to capture both short-term and long-term droughts [39, 40]. The SPI has been integrated into drought monitoring systems at local, regional, and global scales to provide timely information for decision-making and water resource management. In agricultural and water resource management, the SPI is valuable for tasks such as irrigation scheduling, crop yield forecasting, and water allocation decisions [41, 42]. Lotfirad et al. (2022) applied models like SPI and SPEI to predict drought patterns in different climates in Iran, providing valuable insights into future water scarcity [43]. By incorporating SPI-based drought information into decision support systems, stakeholders can optimize water resource management strategies and minimize the negative impacts of drought on agriculture and ecosystems [44–47].

In the context of past research, which has largely overlooked the concurrent impacts of climate change on both agriculture and the tourism industry in the Ardabil Plain, this study assumes a pioneering role. Recognizing the critical significance of wheat production in this region, particularly from the perspective of local officials, the research focuses on wheat as a vital agricultural product. By employing advanced tools, including an ANN model and the SPI, in conjunction with climate scenarios for Iran's northwest between 2040 and 2050, the aim is to bridge the existing knowledge gap. There is currently no existing research that conducts a simultaneous evaluation of the consequences of climate change on water resources, agriculture, and tourism in this area. Furthermore, there is a lack of studies that examine how climate patterns have evolved over time and space and their influence on the livelihoods of the local population. The primary objective remains twofold: first, to comprehensively assess the multifaceted impacts of climate change on both agriculture and tourism, and second, to propose sustainable practices and strategies that address these challenges. This research endeavors to offer a holistic perspective on the region's vulnerabilities and opportunities, aiding local stakeholders and policymakers in making informed decisions to enhance environmental sustainability. Ultimately, the study seeks to ensure the well-being and resilience of the Ardabil Plain's communities in the face of impending climate-related challenges, laying the foundation for a more sustainable and prosperous future.

2. Materials and Methods

2.1. Study Area

This study focuses on the Ardabil Plain in a semi-arid northern Iran region. Geographically, Ardabil province occupies a strategic position for the export of agricultural products, thanks to its shared border with the Republic of Azerbaijan (Figure 1). The Sarein station records the highest annual rainfall in the plain, measuring 370 mm, while the Namin station shows the lowest, with 220.8 mm and a relative humidity of 63.12%. Agriculture and the tourism industry form the primary economic sectors in this basin, which is home to approximately 500,000 people [48–50].

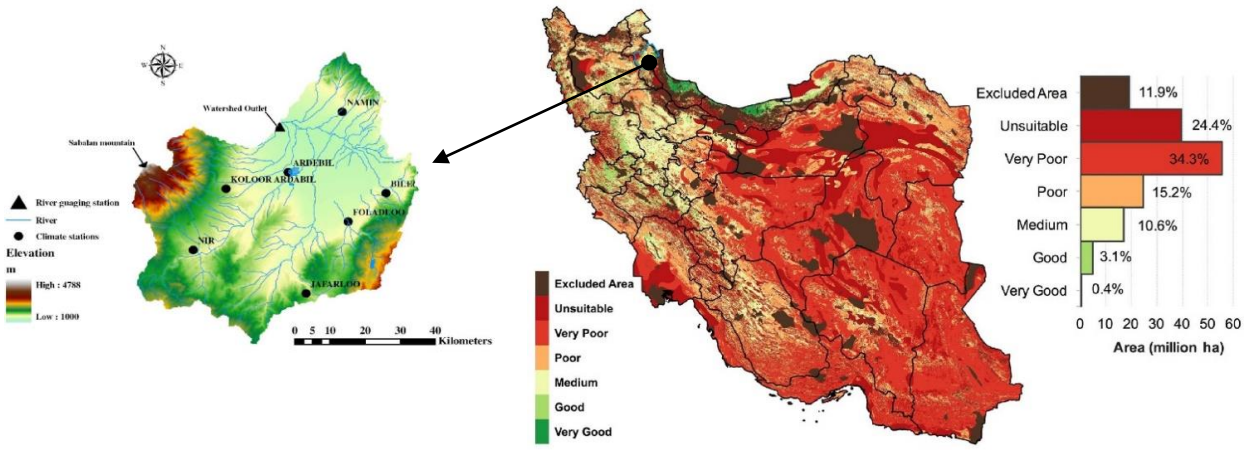

Figure 1. (Right) The agricultural viability of Iran's land, as determined by soil and topographic factors (Mesgaran et al. [51]); and (left) Ardabil Plain

Ardabil province boasts excellent potential for the development of water tourism, thanks to its abundance of hot springs, waterfalls, natural lakes, and constructed dams. With over 110 mineral springs, including 75 thermal springs and 35 cold springs, the region offers a diverse range of aquatic experiences. Over the past two to three decades, the establishment of hydrotherapy complexes and the development of hotels and accommodation centers have significantly contributed to the growth of water tourism, particularly in the city of Sarein. In addition to hot springs and waterfalls, natural lakes such as Neor and Shorabil near Ardabil attract a multitude of tourists from all over the country each year. Shorabil Lake, which has become integrated into the urban fabric of Ardabil in recent years, sees many local residents and visitors flocking to its shores. The lake's surroundings have been enhanced with shopping and accommodation

facilities to cater to the needs of visitors. Mount Sabalan, located in the western part of Ardabil Plain, stands as another prominent tourist attraction. The mountain remains snow-capped for most of the year, making it an ideal destination for snow sports enthusiasts. Ardabil's unique natural features and the development of tourism infrastructure have transformed the province into an appealing destination for water tourism, attracting both domestic and international visitors [48, 52]. To facilitate a more in-depth analysis of the study area, we will partition this plain into three sections. Subsequently, we will assess the economic aspects of agriculture and tourism in these divided regions (Figure 2).

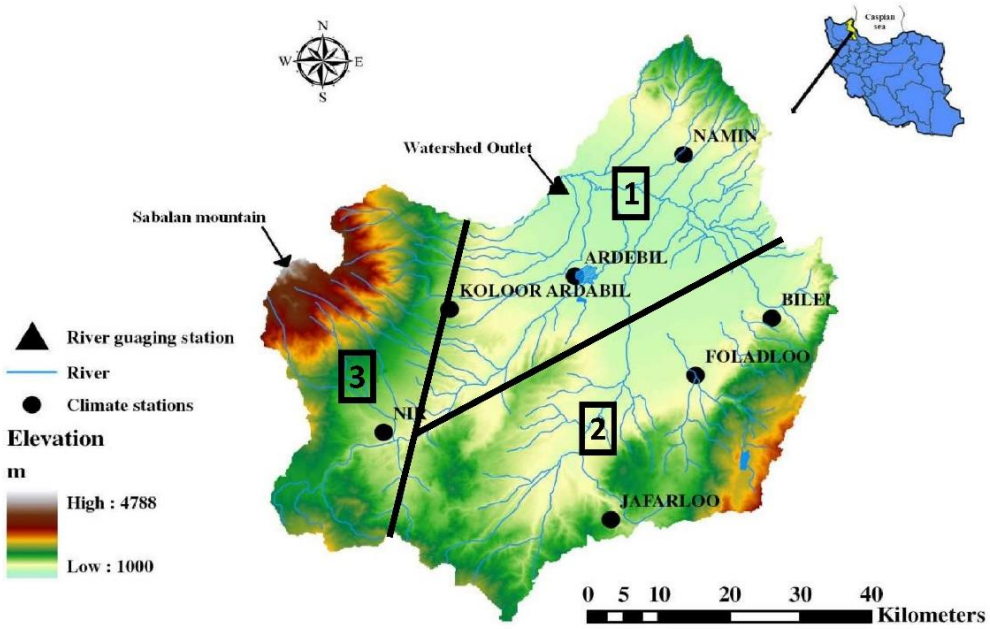

Figure 2. The Ardabil plain map

Ardabil Plain possesses significant capacity to produce various agricultural products. The province holds impressive rankings in several agricultural items, including first in lentil production, second in potato production, third in honey, fifth in sugar beet, and seventh in beans, wheat, and barley. The province has a total of 780,000 hectares of registered agricultural lands, comprising 515,000 hectares of rain-fed lands, 225,000 hectares of non-rain-fed lands, and 40,000 hectares dedicated to horticultural crops. These lands yield approximately 4,500,000 tons of diverse agricultural products [48, 49]. Despite owning slightly over one percent of the country's agricultural land, Ardabil province stands as a pivotal hub for agricultural production in the country. Figure 1 shows the agricultural viability of Iran's land as determined by soil and topographic factors and the location of Ardabil Plain. It contributes more than four percent of the nation's agricultural output within this comparatively smaller area. Currently, the agricultural sector in Ardabil employs 30 percent of the province's workforce, marking the highest employment share among development groups. Table 1 displays the farming areas in this study, measured in hectares. Table 2 provides data regarding the Average Income, Cost, Water Consumption, and Yield per cultivated area for wheat in Ardabil Plain, where wheat comprises over 50 percent of the agricultural activities [53]. Ardabil province's remarkable agricultural performance and advantageous geographical location demonstrate its potential and significance in the agricultural landscape [49]. The province's rich natural resources, combined with the expertise of its farmers, play a vital role in sustaining its agricultural success and contributing to the overall agricultural productivity of the country [51].

Table 1. The Farming Areas in Ardabil province and this Study (hectare)

Attributes	Irrigated Farming Land		Rain-fed Farming Land		Total Farming Land		
	Crop	Garden	Crop	Garden	Irrigated	Rain-fed	Total
Ardabil Province	185,652	30,780	485,218	370	216,432	485,588	702,020
Ardabil Plain	83,156	3,492	148,430	39	86,648	148,469	235,117
Region 1	58,209	2,444	103,901	27	60,654	103,928	164,582
Region 2	24,947	1,048	44,529	12	25,994	44,541	70,535

Table 2. Average income, cost, and water consumption and yield per cultivated area for wheat per hectare of agriculture in Ardabil Plain [53]

Attribute	Income ($)	Cost ($)	Water consumption (m^3)	Production/Area (Total)	Production/Area (Irrigated)	Production/Area (Rain-fed)
Amount	1715.23	709.85	4604/56	1.53	4.25	0.92

2.2. Data

Temperature and rainfall data were collected from seven synoptic stations within the Ardabil Plain. The observed climatic data for the period from 2010 to 2020 were obtained from these seven key synoptic stations in the province. Figure 3 presents the average monthly temperature across all research sites. It is important to note that variations in data from different stations can lead to systematic errors in rain gauge measurements due to factors such as wind, humidity, and evaporation from the gauge's instruments [54, 55]. Despite efforts to establish an extensive network of measurement stations, there will always be areas with no available temperature data [56].

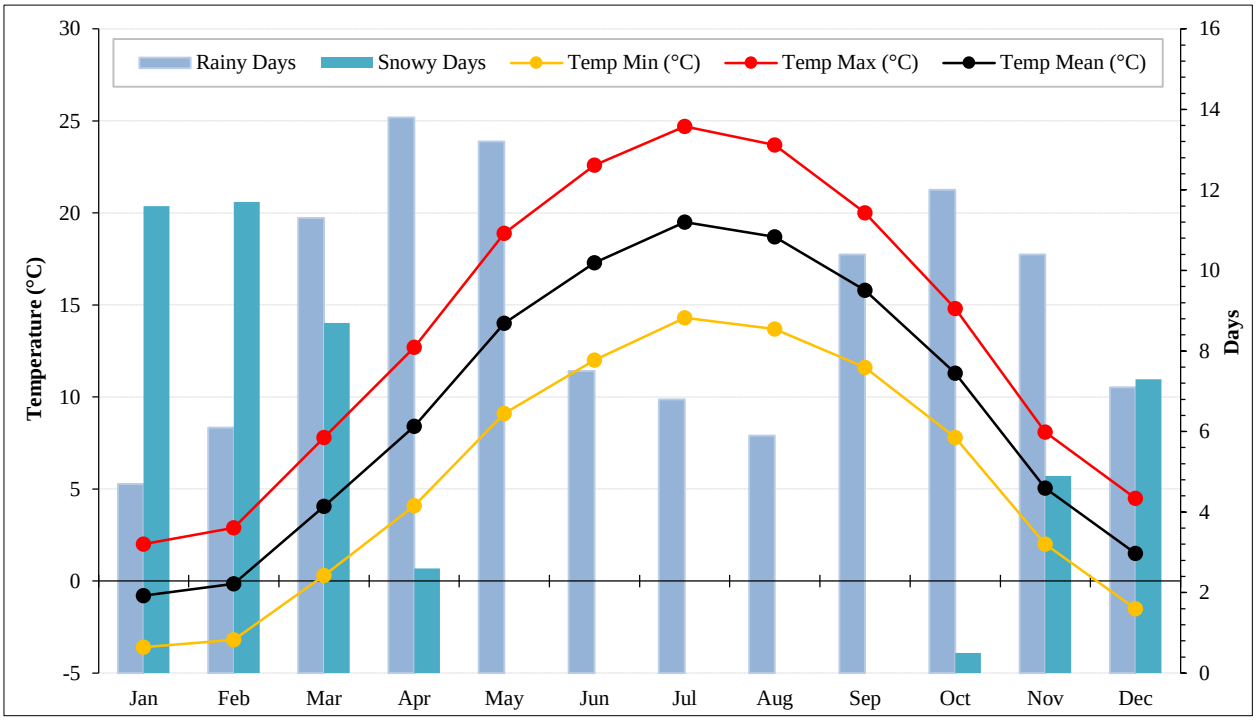

Figure 3. Monthly Temperature and days of precipitation in the Ardabil plain

To estimate future temperature and precipitation patterns, the data from CMIP5 provided by the official website of the Intergovernmental Panel on Climate Change (IPCC) were utilized. This data resource offers raw data from models for past and future climate scenarios at various time periods and conditions. However, one significant drawback of using GCM output is its low resolution, which limits its suitability for regional studies. Consequently, several research institutes have made downscaled versions of GCM output available, providing data on smaller grids to facilitate global access for academic research. In this study, the output from CMIP5 with a grid size of 0.5º×0.5º was used to assess the near-future period of 2040-2050 [57].

3. Research Methods

3.1. Framework Research

The data employed in this study comprises a comprehensive set of hydrology and agriculture data, enabling a multifaceted examination of the Ardabil Plain's environmental dynamics. To project the potential effects of climate change, the research leverages Climate Change Scenarios, specifically the RCP 8.5 scenario, which provides future climate data crucial for predictive analyses. The simulation aspect of the research integrates advanced tools, such as the ANN, facilitating runoff simulations to model changing hydrological patterns. Additionally, the study utilizes the SPI to pinpoint drought periods, offering a critical insight into the region's susceptibility to water scarcity. The core analysis delves into the Climate Change Impact on Agriculture and Tourism, with a particular emphasis on wheat, a pivotal crop for the Ardabil Plain. Meanwhile, the tourism analysis meticulously assesses climatic conditions pertaining to various trip seasons, offering invaluable insights for the tourism industry. Through this multifaceted approach, the study aims to comprehensively evaluate and address the challenges posed by climate change in the Ardabil Plain, ensuring the well-being of its local population and promoting environmental sustainability. The research process flowchart is illustrated in Figure 4.

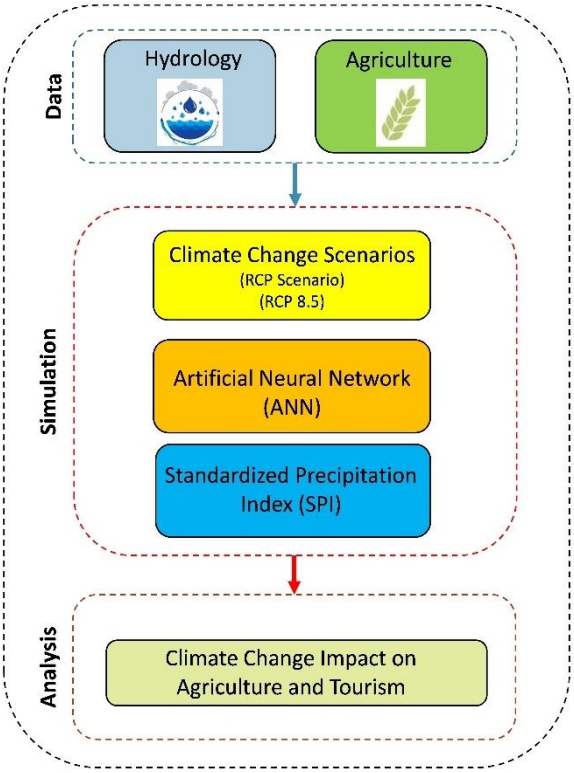

Figure 4. The research process flowchart

In this research, the ANN method was used as a spatial interpolation tool to estimate temperature and precipitation data inflow simulation in Ardabil plain [58-60]. ANN, or Artificial Neural Network, has found applications in hydrology for estimating and predicting hydrological parameters [61-63]. In this study, a specific architecture called Multi-Layer Perceptron (MLP) is used. The MLP consists of interconnected units, also known as perceptrons or neurons, organized in layers including an input layer, an output layer, and potentially one or more hidden layers. The input vector is propagated forward through the network, and the hidden layers employ a nonlinear activation function to linearly combine and transform the input signals. The subsequent layers then utilize the output from the hidden layer as their input. The synaptic weights, which are associated with the connections between neurons and their input channels, represent the linear combinations. It's important to note that an MLP lacks feedback connections, meaning that each layer's neurons are only connected to those in the layer directly preceding it. If the input vector has a dimension of P and the output vector has a dimension of Q, the nonlinear mathematical relationship used to convert the input into the k-th component of the output vector is as follows:

$$out_k = f_{out}(\sum_{j=1}^{M} \lambda_{kj} \leftarrow f_{hid} (\sum_{i=1}^{p} w_{ji} in_i + b_{j0}) + b_{k0}) \quad (1)$$

where w_{ji} is the link weights between unit i of the input layer in and unit j of the hidden layer, λ_{kj} is the link weights between unit j of the hidden layer and unit k of the output layer, b_{k0} and b_{j0} are the bias parameters, M is the number of output hidden units, P is the number of input hidden units, in_i is the input value from the i-th input neuron, out_k is the k-th output unit, and f_{out} and f_{hid} are the activation functions in Equation 1 [64].

3.2. The Standardized Precipitation Index (SPI)

The SPI is widely recognized as a crucial tool for monitoring drought conditions. It stands out among other indicators by considering the element of time. In fact, it can be considered the sole indicator that considers time scales when monitoring dry periods. Determining the appropriate time scale relies on understanding the hydrological impact of drought on various agricultural resources. The time scale can range from one month to several years [65].

To calculate the SPI index, only rainfall data is utilized, focusing solely on the climatic aspect. The monthly rainfall measurements for each station are calculated within the specified time scale. For example, when determining the 3-month scale, the sum of rainfall in April, May, and June is considered as the precipitation index for June. Similarly, the total rainfall in May, June, and July represents the index for the last month in that range. Essentially, for a 3-month scale, the rainfall index for each month is the sum of rainfall in that month and the two preceding months. The cumulative rainfall period is calculated in a similar manner for each month based on the chosen time scale [65].

In the specific study at hand, a 12-month time scale was chosen to examine the effects of drought on agricultural and soil moisture. Once the monthly rainfall values for each station are calculated within the desired time scale, they are fitted into a gamma distribution. Ultimately, this distribution is transformed into a normal distribution using the gamma distribution function and its associated probability density function (PDF).

$$g(x) = \frac{x^{\alpha-1} e^{2\frac{-x}{\beta}}}{\beta^{\alpha}\Gamma(\alpha)} \quad (2)$$

where, the function $g(x)$ represents the probability density function. The variable x signifies the cumulative rainfall for each time scale and every month of the year at each meteorological station. The symbol Γ denotes the gamma function, while α and β represent the shape and scale parameters, respectively. The symbol e in the mathematical expression represents Euler's number. The calculations for Equations 3 and 4 involve these elements [65].

$$\alpha = \frac{1}{4A}(1 + \sqrt{1 + \frac{4A}{3}}) \quad (3)$$

$$\beta = \frac{\bar{X}}{\alpha} \quad (4)$$

The value of A is derived from Equation 5.

$$A = \ln(\overline{X}) - \frac{\sum \ln(x)}{n} \quad (5)$$

Regarding this matter, the variable $\bar{X}$ represents the mean of cumulative rainfall calculated across all comparable instances in each station and at any given time scale. Additionally, x signifies the cumulative rainfall for each time scale in each month. Meanwhile, n represents the count of opposing rainfall occurrences during the same month within the rainy season on any given time scale. As a result, the calculated SPIs for each month within the statistical period are denoted as Z, and they are subsequently normalized [65-67]. Once the index is computed, the drought intensity in the SPI index is determined based on the values presented in Table 3.

Table 3. The categorization of the SPI index to determine the severity of drought and intensity of wetness (McKee et al. [68])

Categories of drought	Values of the SPI indicator
Extremely heavy rainfall	2 ≥
Intense rainfall	1.5–1.99
Moderate rainfall	0.99–1.39
Light rainfall	0.5–0.99
Normal conditions	− 0.39 to 0.39
Mild drought	−0.99 to − 0.5
Moderate drought	− 1.39 to − 1.00
Severe drought	− 1.99 to − 1.50
Extremely severe drought	≤− 2

3.3. Future Projection and Downscaling

Several studies have highlighted the limitations of GCMs due to their coarse resolution and systematic biases [69, 70]. These models struggle to accurately capture regional climate dynamics due to their low resolution, and the biases can become more pronounced when simulating climate change under global warming conditions. To address these issues, bias adjustment is necessary for each model [70] . Downscaling is a technique used to interpolate GCM results to meet local-scale requirements and reduce biases [71] . In this study, the bias-correction change factor approach was employed to scale down the 0.5x0.5 gridded GCMs to the size of weather stations, ensuring higher resolution and preserving the seasonal variability of the observed data [72, 73]. Equations 7 and 8, as proposed by Yang et al., were applied to verify the consistency between the downscaled data mean and the observed data mean using the change factor approach. These equations were used to downscale recorded precipitation and temperature for the projected period of 2040-2050, with the historical reference period being 2010-2020 [70].

$$P_{downscaling\ (m)} = \overline{P_{O_m}} \times \left(\frac{\overline{P_f}}{\overline{P_p}}\right)_m \qquad \text{m = 1, 2, …, 12} \quad (7)$$

$$T_{downscaling\ (m)} = \overline{T_{O_m}} - (\overline{T_{fut}} - \overline{T_{his}})_m \qquad \text{m = 1, 2, …, 12} \quad (8)$$

where, $P_{\text{downscaling (m)}}$ is the projected and downscaled precipitation for a specific month 'm'. It represents the estimated amount of rainfall for that month in the future. $\overline{P_{O_m}}$ is the observed (historical) precipitation for the same month 'm'. It's

the recorded amount of rainfall in the past for that month. $\overline{P_f}$ is a factor representing future precipitation. It's typically derived from climate models and represents the expected changes in precipitation patterns due to climate change. $\overline{P_p}$ is a factor representing past (historical) precipitation. It's used as a reference and is typically calculated as the long-term average of observed precipitation for each month. T $_{\text{downscaling (m)}}$ is the projected and downscaled temperature for a specific month 'm'. It represents the estimated temperature for that month in the future. $\overline{T_{O_m}}$ is the observed (historical) temperature for the same month 'm'. It's the recorded temperature in the past for that month. $\overline{T_{fut}}$ is a factor representing the future temperature. Like P_f, it's derived from climate models and represents the expected changes in temperature due to climate change. $\overline{T_{his}}$ is a factor representing historical temperature. It's typically calculated as the long-term average of observed temperatures for each month [57, 70].

4. Results

4.1. Simulation of Hydrological Parameters

For validation of ANN applied various statistical parameters including Mean Error (ME), Normalized Root Mean Square Error (NRMSE), and Coefficient of Determination (R^2). These parameters were calculated to analyze the outcomes of the techniques by comparing the estimated and measured monthly temperature, precipitation and inflow outlet values. It was observed that the accuracy of the air temperature cross-validations varied from month to month, which could influence the interpolation accuracy for each specific month. The simulation results of the ANN model revealed favorable performance metrics, with an average R^2 value of 0.93. Additionally, the ME and NRMSE values for this model were found to be 1.08 and 0.99, respectively. Overall, the R^2 values for all models indicated satisfactory performance.

In Figure5, the average monthly rainfall is compared between the past eleven-year period and the future eleven-year period. The future rainfall generally shows a decrease compared to the base rainfall throughout the year. The highest decrease in rainfall occurs in October, with a future rainfall of 61.99 mm compared to a base rainfall of 122.42 mm, representing a difference of 60.43 mm. The lowest decrease is observed in June, with a future rainfall of 14.24 mm compared to a base rainfall of 27.98 mm, resulting in a difference of 13.74 mm. It is evident that there will be a decline in rainfall by approximately 38% over the next three decades. The graph highlights that the reduction in rainfall during the autumn months is more significant compared to the rest of the year. Additionally, the decrease in rainfall is relatively equal between the winter and summer months.

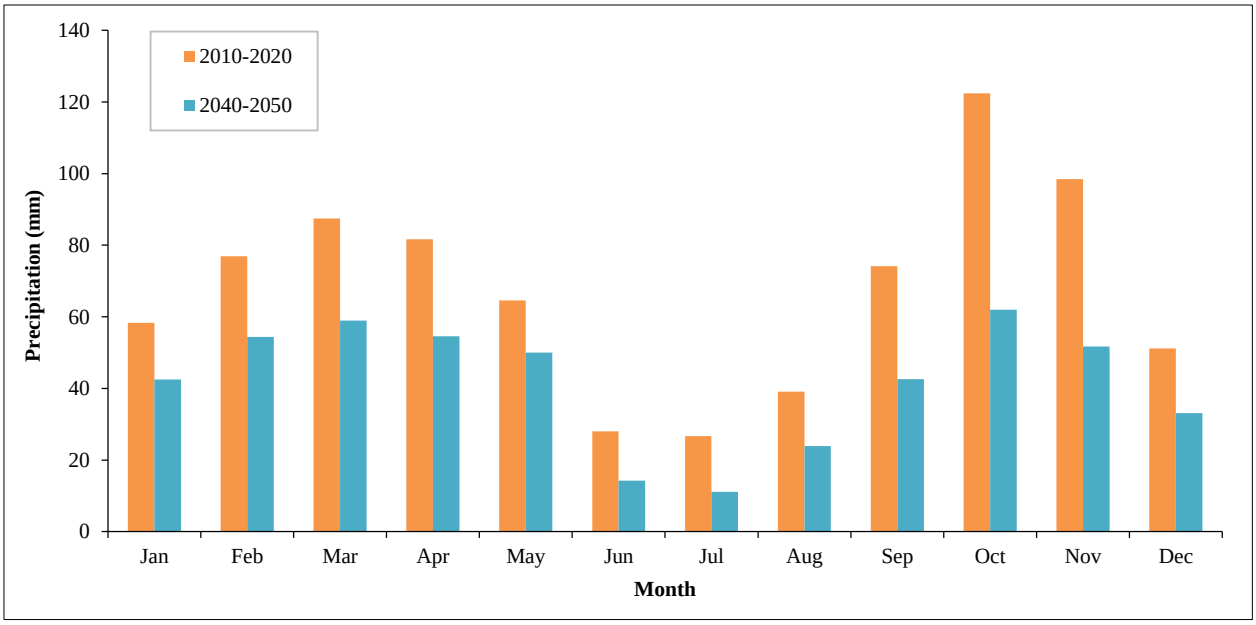

Figure 5. Comparing the average monthly precipitation between a past period and a future period

Figure 6 shows a compression of the average monthly temperature and flow outlet between a past period and a future period. The average base temperature for the year is approximately 9.55°C, while the average future temperature is around 12.46°C. This indicates a significant increase of approximately 2.91°C in the future temperatures compared to the base temperatures with growth 30%. The highest increase in temperature occurs in July, with a future temperature of 23.4°C compared to a base temperature of 19.5°C, representing a difference of 3.9°C. The lowest increase in temperature occurs in January, with a future temperature of 1.2°C compared to a base temperature of –0.8°C, resulting in a difference of 2°C. The average base flow for the year is approximately 28.25 m^3/s, while the average future flow is

around 22 m^3/s, with decreasing 22%. This indicates a decrease of approximately 6.25 m^3/s in the future flow compared to the base flow. The highest flow occurs in April, with a base flow of 52 m^3/s, and the future flow remains relatively similar at 50 m^3/s, indicating a minimal change. The lowest flow occurs in July and August, where both months have no flow at all in the future scenario, while the base flow in July is 6 m^3/s and in August is 3 m^3/s. The data shows that temperatures gradually increase from January to August, and then start to decrease from September to December. In contrast, the water flow decreases from January to August, hitting its lowest points in June, July, and August, and then starts to recover from September to December. The data indicates that Ardabil Plain is vulnerable to water scarcity during certain months, which could have severe implications for agriculture, ecosystems, and the overall environment. The data indicates that Ardabil Plain faces water scarcity during the summer months (June to August) due to reduced flow and lower rainfall. The decrease in flow and rainfall could have adverse effects on agriculture, ecosystems, and water resources availability in the region. In conclusion, the numerical analysis of temperature, flow, and rainfall data in Ardabil Plain suggests a warming trend, decreased flow, and reduced rainfall during certain months. Water scarcity during the drier months poses significant challenges for the region's water resources and agriculture. Implementing sustainable water management practices and monitoring climate change impacts are vital for maintaining a balance between water supply and demand in Ardabil Plain.

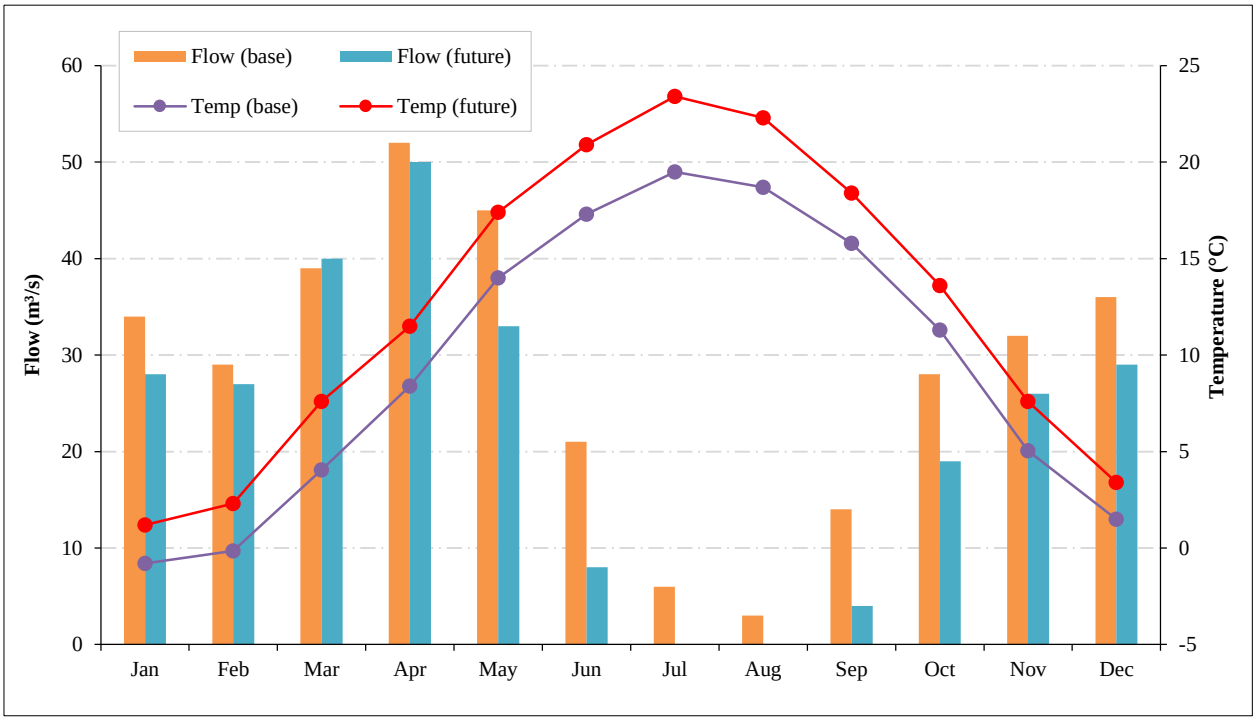

Figure 6. Comparing the average monthly temperature and flow outlet between a past period and a future period

4.2. Future Changes

The ANN model was utilized to generate a spatial dataset representing precipitation and temperature patterns from January to December 2050. As illustrated in Figure 7, monthly temperature patterns based on RCP8.5 scenarios were also generated using ArcGIS software. In January, the temperature pattern reveals the coldest areas in the south (region 2) and west (region 3), with temperatures hovering around -15 ^{0}C. However, by February, noticeable cold is primarily concentrated in the southeast portion of the plain (region 2). This temperature trend persists in Ardabil until May, with April serving as the transition month, exhibiting temperatures ranging from 0 to 15 ^{0}C. April marks the midpoint of spring in this region. Come May, high temperatures dominate the northwest area, gradually diminishing towards the eastern basin. Over the subsequent three months, June, July, and August, temperatures experience a consistent rise, maintaining an average of approximately 27 ^{0}C across the plain. As September and October roll in, a cooling trend becomes evident in the southern and western regions of the basin, with temperatures spanning from -1 to 22 ^{0}C. November presents a significant temperature drop in region 2 of the Ardabil plain, contrasting sharply with the northern regions of the basin, where temperatures plummet from 10 to -15 ^{0}C. December, one of the coldest months in Ardabil plain, ushers in uniform cold throughout the northern regions. The study predicts an overall increase in the average temperature for all months compared to the observed period, particularly under the RCP8.5 scenario where temperatures exceed past data values.

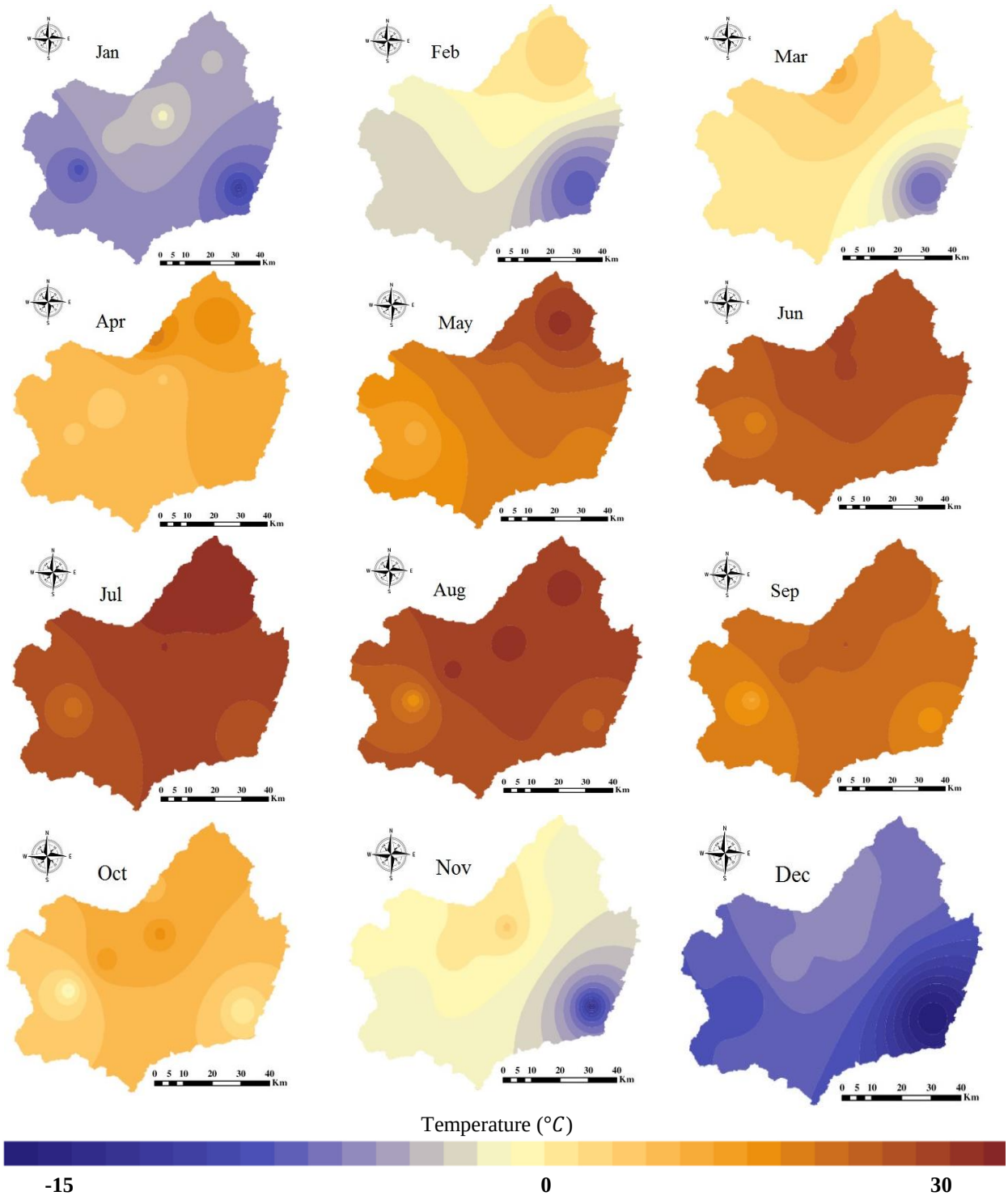

Figure 7. Mean monthly temperature of the Ardabil plain in 2040

Figure 8 provides a spatial representation of the anticipated seasonal precipitation variations in the Ardabil plain in the near future that making with RCP8.5 scenario. In terms of rainfall patterns, January's data indicates reduced precipitation in the central parts of Ardabil plain. February witnesses an uptick in rainfall, particularly in the western regions (region 3) of the basin, with precipitation levels ranging from 5 to 120 mm during these two months. March showcases nearly uniform rainfall across the basin. April and May stand out as months with the highest precipitation, especially in May when central and western regions of the basin, as well as some areas in the south (region 2), experience the greatest rainfall, varying between approximately 20 and 220 mm during these two months. Starting from June, a declining trend in rainfall becomes apparent, reaching near-zero levels in August and September. Come October, rainfall emerges across most areas, with the western region (region 3) receiving more significant amounts, ranging from around 10 to 130 mm in the northern part of the basin. November marks a resurgence of rain in the Ardabil plain, particularly in the southern and western regions. December sees a return to uniform rainfall patterns across most parts of the plain, completing the annual climatic cycle.

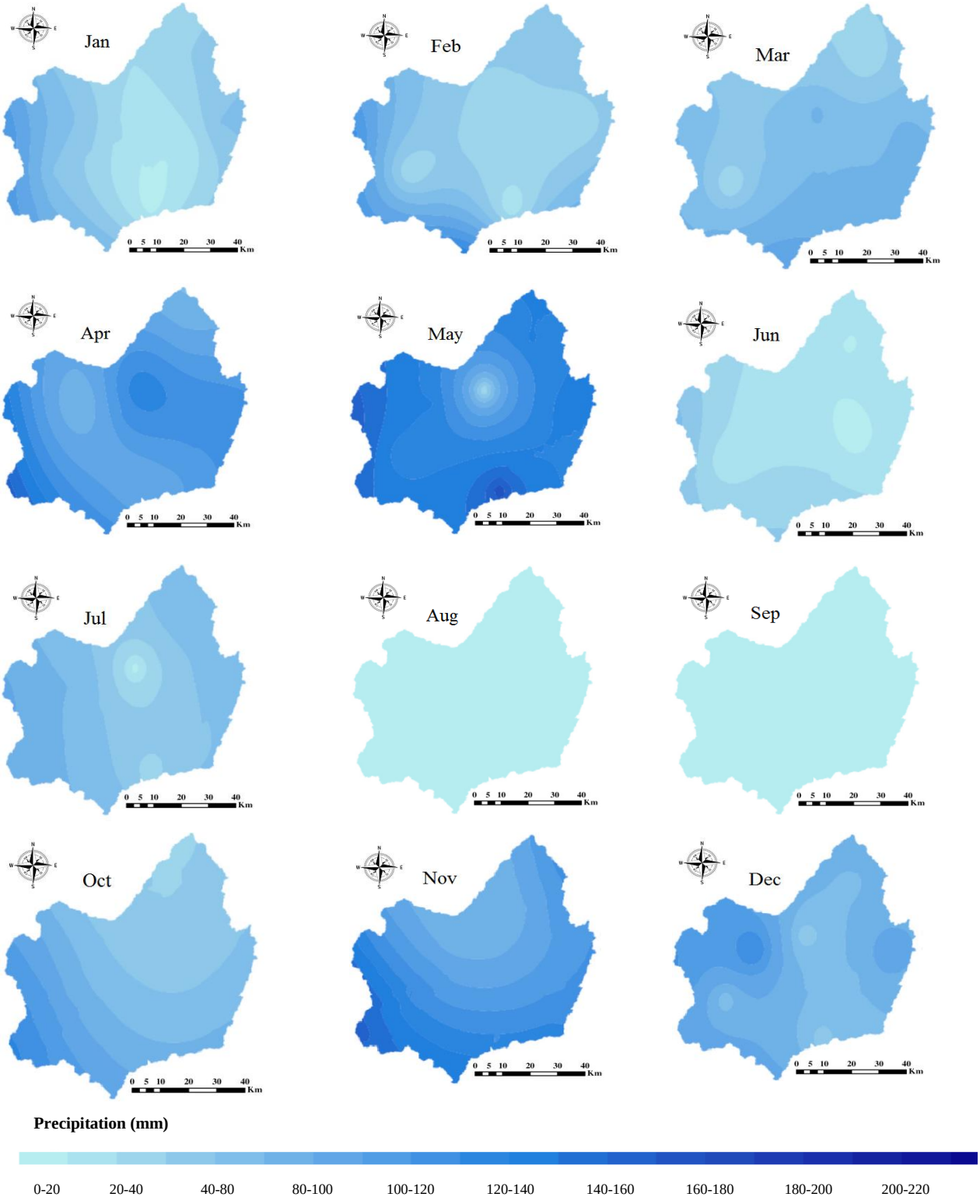

Figure 8. Maximum monthly precipitation of the Ardabil plain

4.3. SPI Results

The data provided in Tables 4 and 5 offers a comprehensive view of drought patterns in Ardabil, utilizing the Standardized Precipitation Index (SPI) on a 12-month scale. SPI serves as a crucial tool for assessing and quantifying drought severity, providing valuable information about the region's climatic conditions during two distinct time periods: 2010-2020 and 2040-2050.

In the historical dataset spanning from 2010 to 2020 (Table 4), Ardabil's climate exhibited a dynamic range of drought conditions. Throughout this decade, the SPI values varied, showcasing the region's susceptibility to fluctuations in precipitation. Notably, the year 2011 stood out with an SPI of 1.42, representing "Moderate rainfall," indicating favorable precipitation levels. Conversely, the year 2017 experienced "Moderate drought," marked by an SPI of -1.12,

signifying below-average rainfall. Between 2013 and 2015, Ardabil enjoyed a period of "Normal conditions," marked by SPI values hovering around zero, indicating balanced precipitation levels. In essence, this decade presented a diverse range of drought scenarios, encompassing mild droughts, moderate rainfall, and extended periods of "Normal conditions."

Table 4. The SPI index on a 12-month scale used to assess the drought levels in Ardabil between 2010 and 2020

Year	SPI	Categories of drought
2010	-0.98	Mild drought
2011	1.42	Moderate rainfall
2012	-0.98	Mild drought
2013	-0.05	Normal conditions
2014	-0.25	Normal conditions
2015	0.14	Normal conditions
2016	1.49	Moderate rainfall
2017	-1.12	Moderate drought
2018	0.36	Normal conditions
2019	-0.03	Normal conditions
2020	0.88	Light rainfall

Table 5. The SPI index on a 12-month scale used to assess the drought levels in Ardabil between 2040 and 2050

Year	SPI	Categories of drought
2040	-0.48	Normal conditions
2041	0.08	Normal conditions
2042	-0.80	Mild drought
2043	0.19	Normal conditions
2044	-0.72	Mild drought
2045	-0.62	Mild drought
2046	-0.13	Normal conditions
2047	-0.37	Normal conditions
2048	-0.70	Mild drought
2049	-0.92	Mild drought
2050	-1.16	Moderate drought

Contrastingly, the future projection for the years 2040 to 2050 (Table 5) offers insights into the evolving drought patterns expected in Ardabil. This projection begins with two years of "Normal conditions" in 2040 and 2041, where SPI values approach zero, suggesting an equilibrium in precipitation levels. However, starting from 2042, a shift towards milder drought conditions becomes apparent, as indicated by consistently negative SPI values. An exception occurs in 2043, marked by "Normal conditions." The most striking observation in this projection is the year 2050, categorized as "Moderate drought," with an SPI of -1.16, suggesting a significant reduction in precipitation. While sporadic instances of "Normal conditions" are observed, the prevailing trend in this decade leans towards mild drought conditions.

Comparing these two datasets, it becomes evident that the temporal context plays a pivotal role in understanding Ardabil's drought dynamics. Table 4, representing historical data from 2010 to 2020, reveals a decade marked by varying drought intensities. Conversely, Table 5, offering projections for 2040 to 2050, indicates a shift towards milder drought conditions, with "Normal conditions" becoming less frequent in the latter half of the decade. This contrast underscores the likelihood of increased drought challenges facing Ardabil in the coming years, as reflected in the higher prevalence of mild and moderate droughts in the 2040-2050 projection.

4.4. Agriculture Analysis

Approximately 58% of the agricultural land in Ardabil Plain is dedicated to cultivating wheat, a staple food for both the people of Iran and the broader region. This section discusses the production, profitability, and potential losses resulting from climate change on this critical crop in the area. For this analysis, it is assumed that all other factors affecting wheat production will remain constant in the future, except for the amount of rainfall and water used for irrigation in wheat cultivation. Figure 9 illustrates a general trend of decreasing wheat production volume in proportion

to its cultivation area. Specifically, for irrigated lands, the production value is expected to decline from 4.25 to 3.32, while for rain-fed lands, it will decrease from 0.92 to 0.57.

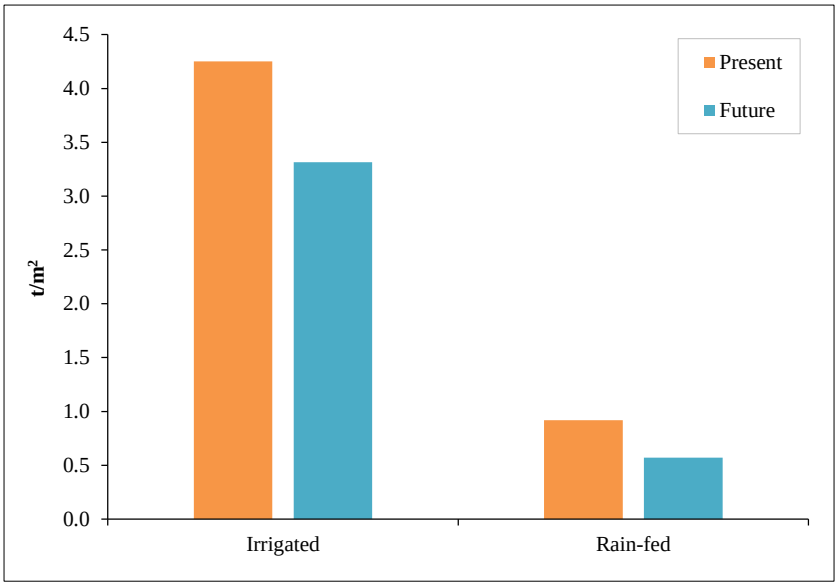

Figure 9. Comparison amount of wheat production to area farming land for two period present and future

Table 6 displays the production volume and alterations in wheat production between the present and future periods. Overall, there is a notable decline in production volume, particularly in a specific region of Ardabil Plain. In the present scenario, Ardabil Plain produces a total of 284,182 tons of wheat, with 204,980 tons from irrigated crops and 79,202 tons from rain-fed crops. In the future scenario, the total wheat production is projected to decrease to 209,196 tons, with 160,125 tons from irrigated crops and 49,071 tons from rain-fed crops. Both irrigated and rain-fed wheat productions show a significant decrease in the future. In the case of irrigated crops, there is a reduction of 44,854 tons, and for rain-fed crops, there is a reduction of 30,131 tons.

Table 6. Amount of Wheat Production in the Ardabil Plain at present period and future period (ton)

Attributes	Present		Future		Changing Productions		
	Irrigated	Rain-fed	Irrigated	Rain-fed	Irrigated	Rain-fed	Total
Ardabil Plain	204,980	79,202	160,125	49,071	-44,854	-30,131	-74,986
Region 1	143,486	55,442	112,088	34,350	-31,398	-21,092	-52,490
Region 2	61,494	23,761	48,038	14,721	-13,456	-9,039	-22,496

Based on the information provided in Table 2, to calculate the net income from wheat production, you need to multiply the volume of wheat production by the value of $1005.38 US dollars. This will give you the amount of losses incurred due to climate change for wheat production. The data also indicates the projected net income changes resulting from the decrease in wheat production in both present and future scenarios. In the future, the total net income will be lost for wheat production, around -$75,389,059, with -$45,095,663 from irrigated crops and -$30,293,396 from rain-fed crops. In the future scenario, the total net income in region 1 is projected to decrease to -$52,772,341, with -$31,566,964 from irrigated crops and -$21,205,377 from rain-fed crops. Similarly, in region 2, both irrigated and rain-fed crops show a decrease in net income of around -$ 22,617,028. In the case of irrigated crops, there is a decrease of $13,528,699, and for rain-fed crops, there is a decrease of $9,088,019.

4.5. Tourism Status in the Future

Regarding the net income status of tourism industry, specific details have not been provided for this area. However, considering the future climate conditions, particularly in the 3rd region of Ardabil Plain, it can be determined whether the area is suitable or unsuitable for tourists. Aminiania et al. categorized the Ardabil province into three statuses with characteristics suitable, average, and unsuitable for tourism [18].

With attention Figure 7, in the spring months, from March to May, temperatures vary widely between region 1 and region 3, ranging from 0.5 ^{0}C in mountainous regions to a warm 30 ^{0}C in lowlands. Spring emerges as a favorable season for tourism, with lowlands being particularly inviting, while May's increasing heat can discourage travel to foothill areas. Summer, spanning June to August, sees most regions in the Ardabil plain with temperatures above 15 ^{0}C. However,

region 1 and part of region 3 become less conducive to tourism due to unfavorable temperatures, while mountainous regions remain relatively attractive. In autumn, September's warmth, around 26 ^{0}C in the north, might deter tourists, but October and November bring a significant temperature drop, making November the preferred autumn travel month, particularly in the south. Finally, winter, from December to February, brings cold temperatures, averaging between -1 and -15 ^{0}C across most regions. Despite the chill, the presence of hot springs sustains tourism, especially in February when certain northern areas offer more pleasant temperatures. These temperature fluctuations influence the choice of travel months for tourists in Ardabil.

According to their findings the west of Ardabil Plain (section 3 of Figure 2) demonstrated suitable conditions for tourists based on temperature and weather conditions in the spring and summer months over a twenty-year period until 2019 [74]. However, concerning SPI, which indicated normal conditions during the base period, projections show that the SPI will display moderate drought conditions in 2050. This suggests that the region may face unsuitable conditions for tourism in the future in the spring and summer months, presenting a concerning outlook for officials and individuals in the tourism industry of the province. There is a potential risk of unemployment and reduced revenue in the tourism sector due to this prediction.

5. Discussion

The information provided presents a comprehensive analysis of various factors impacting the Ardabil region, including climate change effects, water availability, agricultural productivity, and the tourism industry. The analysis highlights the potential challenges and implications that the region may face in the near future. The Ardabil region is projected to experience rising temperatures and changing rainfall patterns over the next three decades. This will have significant implications for agriculture, water availability, and the tourism industry. Region 1 (north of the plain) will face higher temperature increases, posing challenges for farmers. In contrast, Region 2 (south of the plain) may become more suitable for agriculture due to higher precipitation levels. However, the melting of snow on Sablan mountain peak during the spring season in Region 3, a beloved tourist attraction, is currently at risk, and the increasing temperature might not be suitable for tourists during the summer. The analysis shows a 38% decline in rainfall, particularly during autumn, and a potential shift in precipitation timing and intensity. The situation is far from optimal, as the Ardabil plain alone contributes to approximately 45% of the irrigated crops and 30% of the rain-fed crops in Ardabil province. The majority of rain-fed crops (nearly 70% rain-fed) in Region 1 face significant challenges, causing farmers to encounter serious issues. Given the focus on the region's primary crop, which is wheat, and considering the significant water consumption associated with wheat cultivation, it is projected that wheat production in the region may experience a decrease of approximately 26%. The potential decline in net income from wheat production in the near future is concerning for the region. The projected total net income loss for wheat production is estimated to be approximately -$75,389,059.

The findings suggest that the availability of water sources in regions 2 and 3 may result in a shift in population density towards these areas in the future. This demographic change could have significant financial and social implications, some of which may be irreversible. Firstly, the agricultural infrastructure in Region 2 is ill-equipped to handle a large influx of people. Secondly, this migration may lead to the separation of families due to the limited capacity of smaller communities in the South. Nevertheless, it is important to acknowledge the potential risks of floods in the western areas (region 3) due to rising maximum temperatures compared to the current period. This is particularly concerning because part of this region comprises snow-covered mountains, which can contribute to the exacerbation of natural disasters like floods. These floods not only pose threats to human health but also have the potential to create an unemployment crisis in the tourism industry. Furthermore, the rise in temperature in the future will lead to unfavorable conditions, particularly in Region 3. This is concerning for the residents of the region, as their primary livelihoods rely heavily on tourism.

To address these issues, it will be crucial for farmers to relocate agricultural lands from region 1 to region 2 and adopt sustainable farming practices. In order to tackle this challenge, stakeholders should take several measures. Firstly, infrastructure improvements should be undertaken to support the relocation process and ensure the smooth transition of agricultural activities. Secondly, proactive communication among all relevant parties is necessary to facilitate coordination and collaboration during the relocation process. Lastly, early investments in advanced irrigation systems are essential to adapt to changing conditions and ensure the successful establishment of sustainable farming practices in Region 2. Furthermore, the changes in temperature and rainfall patterns in the Ardabil region have significant economic implications for the entire country. Given the region's heavy reliance on agriculture and tourism, the potential economic consequences of climate change in Ardabil are significant. Addressing these challenges requires comprehensive strategies that focus on sustainable agricultural practices, efficient water resource management, and measures to preserve and enhance the region's tourist attractions. Additionally, investment in diversifying the local economy, exploring alternative sources of income, and promoting employment opportunities in other sectors can help mitigate the economic risks associated with climate change in Ardabil, ensuring the region's long-term economic stability and growth.

6. Conclusion

This study aims to enhance environmental sustainability in a critical region by identifying areas prone to drought in the near future with an ANN model that was used to determine the optimal method for interpolating monthly temperature and precipitation data. Using ArcGIS software, monthly temperature patterns for the Ardabil basin in 2050 were generated, and the severity of the drought was evaluated using SPI. The results showed favorable performance metrics for the ANN model, with an average R^2 value of 0.93, indicating a high level of accuracy. The analysis of future climate scenarios indicates a significant increase in temperature across all months. Particularly under the RCP8.5 scenario, temperatures are projected to rise, with variations observed across different regions of the Ardabil plain. Additionally, there is a noticeable decrease in rainfall, with the autumn months experiencing the most significant reductions. For the analysis of crops as a sample, wheat production, a staple crop in the region, is projected to decrease due to changing precipitation patterns and increased temperatures. Irrigated and rain-fed wheat production is expected to decline, with potential losses in net income for farmers estimated at approximately -$75,389,059. The decline in rainfall and changing precipitation patterns pose a risk to water resources in the Ardabil region. The analysis suggests a potential shift in population density towards areas with more accessible water sources, which could have socio-economic implications. The tourism industry in the region may face challenges due to rising temperatures and shifting climate conditions. Areas that were previously suitable for tourism may become less attractive, potentially impacting local economies and employment. The SPI analysis reveals evolving drought patterns. While the historical period from 2010 to 2020 exhibited varying drought conditions, the projection for 2040 to 2050 suggests an increase in mild and moderate droughts, highlighting the changing climatic conditions. To address these challenges, it is imperative to implement sustainable water management practices, monitor climate change impacts, and adapt agricultural strategies to the evolving climate. Furthermore, efforts to diversify the local economy and create employment opportunities outside of the agriculture and tourism sectors will be vital for the long-term stability and growth of the Ardabil region.

In pursuit of advancing environmental sustainability in the Ardabil region, this study has unearthed critical insights into the impending challenges climate change poses. While the current findings provide a comprehensive overview of the region's future, there are exciting avenues for further research and action. One promising direction is using agent-based models. This powerful tool can simulate complex climate adaptation scenarios, facilitating a deeper understanding of the dynamic interactions between environmental, social, and economic factors. By incorporating agent-based models into future research, we can explore innovative strategies and policies that harness the collective efforts of various stakeholders, fostering adaptive responses to the evolving climate landscape. Looking ahead, it becomes evident that Ardabil's journey towards climate resilience demands multifaceted solutions. The region must embark on proactive measures, starting with climate-resilient agriculture that encompasses drought-resistant crop varieties, precision farming technologies, and efficient irrigation practices. Water resource management remains paramount, necessitating intelligent water conservation and sustainable groundwater governance. Diversifying the tourism sector through cultural, eco, and adventure tourism can mitigate reliance on climate-sensitive offerings. In contrast, economic diversification into sectors such as renewable energy and technology ventures can enhance overall resilience. Community engagement and education programs empower locals to actively participate in climate resilience initiatives, while international collaborations offer valuable resources and insights. Continuous climate monitoring and research will guide informed decision-making and adaptive strategies.

7. Declarations

7.1. Author Contributions

Conceptualization, K.J. and M.M.; methodology, K.J.; software, K.J.; validation, K.J., A.A. and J.Z.; formal analysis, K.J.; investigation, K.J.; resources, M.D.; data curation, K.J.; writing—original draft preparation, K.J.; writing—review and editing, S.H.; visualization, S.H.; supervision, A.A.; project administration, M.M.; funding acquisition, A.A. All authors have read and agreed to the published version of the manuscript.

7.2. Data Availability Statement

Data sharing is not applicable to this article.

7.3. Funding

The authors received no financial support for the research, authorship, and/or publication of this article.

7.4. Conflicts of Interest

The authors declare no conflict of interest.

8. References

[1] SafarianZengir, V., Sobhani, B., & Asghari, S. (2020). Modeling and Monitoring of Drought for forecasting it, to Reduce Natural hazards Atmosphere in western and north western part of Iran, Iran. Air Quality, Atmosphere & Health, 13(1), 119–130. doi:10.1007/s11869-019-00776-8.

[2] Ozturk, T., Altinsoy, H., Türkeş, M., & Kurnaz, M. L. (2012). Simulation of temperature and precipitation climatology for the Central Asia CORDEX domain using RegCM 4.0. Climate Research, 52(1), 63–76. doi:10.3354/cr01082.

[3] Toosi, A.S., Calbimonte, G. H., Nouri, H., & Alaghmand, S. (2019). River basin-scale flood hazard assessment using a modified multi-criteria decision analysis approach: A case study. Journal of Hydrology, 574, 660–671. doi:10.1016/j.jhydrol.2019.04.072.

[4] Vaghefi, S. A., Keykhai, M., Jahanbakhshi, F., Sheikholeslami, J., Ahmadi, A., Yang, H., & Abbaspour, K. C. (2019). The future of extreme climate in Iran. Scientific Reports, 9(1), 1464. doi:10.1038/s41598-018-38071-8.

[5] Yazdani, M. H., Amininia, K., Safarianzengir, V., Soltani, N., & parhizkar, H. (2021). Analyzing climate change and its effects on drought and water scarcity (case study: Ardabil, Northwestern Province of Iran, Iran). Sustainable Water Resources Management, 7(2), 7. doi:10.1007/s40899-021-00494-z.

[6] Ghorbani, M. A., Mahmoud Alilou, S., Javidan, S., & Naganna, S. R. (2021). Assessment of spatio-temporal variability of rainfall and mean air temperature over Ardabil province, Iran. SN Applied Sciences, 3(8). doi:10.1007/s42452-021-04698-y.

[7] Barati, A. A., Azadi, H., Movahhed Moghaddam, S., Scheffran, J., & Dehghani Pour, M. (2023). Agricultural expansion and its impacts on climate change: evidence from Iran. Environment, Development and Sustainability. doi:10.1007/s10668-023-02926-6.

[8] Hamedi, H., Alesheikh, A. A., Panahi, M., & Lee, S. (2022). Landslide susceptibility mapping using deep learning models in Ardabil province, Iran. Stochastic Environmental Research and Risk Assessment, 36(12), 4287–4310. doi:10.1007/s00477-022-02263-6.

[9] Kuriachen, P., Korekallu Srinivasa, A., Sam, A. S., & Surendran Padmaja, S. (2022). The Economics of Climate Change in Agriculture. Innovative Approaches for Sustainable Development. Springer, Cham, Switzerland. doi:10.1007/978-3-030-90549-1_1.

[10] Fatahi, A., Safarian Zengir, V., Sobhani, B., Kianian, M., & Ghahremani, A. (2022). Assessment and zoning of suitable climate for economic development of cultivation of Sunflower (Helianthus annuus) garden crop (Ardabil Province, Iran). European Journal of Horticultural Science, 87(1), 1–12. doi:10.17660/eJHS.2022/001.

[11] Ghanbari, R., Sobhani, B., Aghaee, M., oshnooei nooshabadi, A., & Safarianzengir, V. (2021). Monitoring and evaluation of effective climate parameters on the cultivation and zoning of corn agricultural crop in Iran (case study: Ardabil province). Arabian Journal of Geosciences, 14(5), 1–11. doi:10.1007/s12517-021-06807-y.

[12] Deihimfard, R., Rahimi-Moghaddam, S., Collins, B., & Azizi, K. (2022). Future climate change could reduce irrigated and rainfed wheat water footprint in arid environments. Science of the Total Environment, 807, 150991. doi:10.1016/j.scitotenv.2021.150991.

[13] Satari, S.Y., & Khalilian, S. (2020). On Projecting Climate Change Impacts on Soybean Yield in Iran: An Econometric Approach. Environmental Processes, 7(1), 73–87. doi:10.1007/s40710-019-00400-y.

[14] Tayyebi, M., Sharafati, A., Nazif, S., & Raziei, T. (2023). Assessment of adaptation scenarios for agriculture water allocation under climate change impact. Stochastic Environmental Research and Risk Assessment, 37(9), 3527–3549. doi:10.1007/s00477-023-02467-4.

[15] Bahlool, Q. (2023). Tourist Attractions in Badakhshan Province, Its Role in the Local Economy. Integrated Journal for Research in Arts and Humanities, 3(1), 23–29. doi:10.55544/ijrah.3.1.5.

[16] Roshan, G., Yousefi, R., & Fitchett, J. M. (2016). Long-term trends in tourism climate index scores for 40 stations across Iran: the role of climate change and influence on tourism sustainability. International Journal of Biometeorology, 60(1), 33–52. doi:10.1007/s00484-015-1003-0.

[17] Sobhani, B., & Safarian, V. Z. (2020). Evaluation and zoning of environmental climatic parameters for tourism feasibility in northwestern Iran, located on the western border of Turkey. Modeling Earth Systems and Environment, 6(2), 853–864. doi:10.1007/s40808-020-00712-1.

[18] Amininia, K., Abad, B., Safarianzengir, V., GhaffariGilandeh, A., & Sobhani, B. (2020). Investigation and analysis of climate comfort on people health tourism in Ardabil province, Iran. Air Quality, Atmosphere & Health, 13(11), 1293–1303. doi:10.1007/s11869-020-00883-x.

[19] Arami Shamasbi, F., Kanooni, A., & Rasinezami, S. (2022). The effect of different management scenarios on quantitative changes in water resources of Balekhlichai river watershed and Ardabil plain aquifer using MODSIM model. Water and Irrigation Management, 11(4), 923–935.

[20] Javan, K., Saleh, F. N., & Shahraiyni, H. T. (2013). The Influences of Climate Change on the Runoff of Gharehsoo River Watershed. American Journal of Climate Change, 2(4), 296–305. doi:10.4236/ajcc.2013.24030.

[21] Najjar Ghabel, S., Zarghami, M., Akhbari, M., & Nadiri, A. A. (2019). Groundwater management in Ardabil plain using agent-based modeling. Iran-Water Resources Research, 15(3), 1-16. (In Persian).

[22] Araste, M., Kaboli, H., & Yazdani, M. (2017). Assessing the impacts of meteorological drought on yield of rainfed wheat and barley (Case study: Khorasan Razavi province). Journal of Agricultural Meteorology, 5(1), 15-25. doi:10.22125/AGMJ.2017.54980.

[23] Emadodin, I., Reinsch, T., & Taube, F. (2019). Drought and desertification in Iran. Hydrology, 6(3), 66. doi:10.3390/hydrology6030066.

[24] Nourani, V., Ghareh Tapeh, A. H., Khodkar, K., & Huang, J. J. (2023). Assessing long-term climate change impact on spatiotemporal changes of groundwater level using autoregressive-based and ensemble machine learning models. Journal of Environmental Management, 336, 117653. doi:10.1016/j.jenvman.2023.117653.

[25] Nouri-Khajebelagh, R., Khaledian, M., & Kavoosi-Kalashami, M. (2022). Determination of global water value to improve water management in Ardabil plain, Iran. Acta Geophysica, 70(2), 791–799. doi:10.1007/s11600-022-00741-7.

[26] Anaraki, M. V., Farzin, S., Mousavi, S. F., & Karami, H. (2021). Uncertainty Analysis of Climate Change Impacts on Flood Frequency by Using Hybrid Machine Learning Methods. Water Resources Management, 35(1), 199–223. doi:10.1007/s11269-020-02719-w.

[27] Appelhans, T., Mwangomo, E., Hardy, D. R., Hemp, A., & Nauss, T. (2015). Evaluating machine learning approaches for the interpolation of monthly air temperature at Mt. Kilimanjaro, Tanzania. Spatial Statistics, 14, 91–113. doi:10.1016/j.spasta.2015.05.008.

[28] El-Mahdy, M. E. S., El-Abd, W. A., & Morsi, F. I. (2021). Forecasting lake evaporation under a changing climate with an integrated artificial neural network model: A case study Lake Nasser, Egypt. Journal of African Earth Sciences, 179, 104191. doi:10.1016/j.jafrearsci.2021.104191.

[29] Amirhossien, F., Alireza, F., Kazem, J., & Mohammadbagher, S. (2015). A Comparison of ANN and HSPF Models for Runoff Simulation in Balkhichai River Watershed, Iran. American Journal of Climate Change, 4(3), 203–216. doi:10.4236/ajcc.2015.43016.

[30] Javan, K., Lialestani, M. R. F. H., Ashouri, H., & Moosavian, N. (2015). Assessment of the impacts of nonstationarity on watershed runoff using artificial neural networks: a case study in Ardebil, Iran. Modeling Earth Systems and Environment, 1(3), 1–10. doi:10.1007/s40808-015-0030-5.

[31] Luk, K. C., Ball, J. E., & Sharma, A. (2000). A study of optimal model lag and spatial inputs to artificial neural network for rainfall forecasting. Journal of Hydrology, 227(1–4), 56–65. doi:10.1016/S0022-1694(99)00165-1.

[32] Alasali, F., Tawalbeh, R., Ghanem, Z., Mohammad, F., & Alghazzawi, M. (2021). A sustainable early warning system using rolling forecasts based on ANN and golden ratio optimization methods to accurately predict real-time water levels and flash flood. Sensors, 21(13), 4598. doi:10.3390/s21134598.

[33] Balist, J., Malekmohammadi, B., Jafari, H. R., Nohegar, A., & Geneletti, D. (2022). Detecting land use and climate impacts on water yield ecosystem service in arid and semi-arid areas. A study in Sirvan River Basin-Iran. Applied Water Science, 12(1), 1–14. doi:10.1007/s13201-021-01545-8.

[34] Dhamodaran, S., & Lakshmi, M. (2021). Comparative analysis of spatial interpolation with climatic changes using inverse distance method. Journal of Ambient Intelligence and Humanized Computing, 12(6), 6725–6734. doi:10.1007/s12652-020-02296-1.

[35] Taie Semiromi, M., & Koch, M. (2019). Analysis of spatio-temporal variability of surface–groundwater interactions in the Gharehsoo river basin, Iran, using a coupled SWAT-MODFLOW model. Environmental Earth Sciences, 78(6), 1–21. doi:10.1007/s12665-019-8206-3.

[36] Anshuka, A., van Ogtrop, F. F., & Willem Vervoort, R. (2019). Drought forecasting through statistical models using standardised precipitation index: a systematic review and meta-regression analysis. Natural Hazards, 97(2), 955–977. doi:10.1007/s11069-019-03665-6.

[37] Naresh Kumar, M., Murthy, C. S., Sesha sai, M. V. R., & Roy, P. S. (2009). On the use of Standardized Precipitation Index (SPI) for drought intensity assessment. Meteorological Applications, 16(3), 381–389. doi:10.1002/met.136.

[38] Wang, Q., Zhang, R., Qi, J., Zeng, J., Wu, J., Shui, W., Wu, X., & Li, J. (2022). An improved daily standardized precipitation index dataset for mainland China from 1961 to 2018. Scientific Data, 9(1), 124. doi:10.1038/s41597-022-01201-z.

[39] Dikshit, A., Pradhan, B., & Alamri, A. M. (2020). Short-term spatio-temporal drought forecasting using random forests model at New South Wales, Australia. Applied Sciences (Switzerland), 10(12), 4254. doi:10.3390/app10124254.

[40] Farahmand, A., & AghaKouchak, A. (2015). A generalized framework for deriving nonparametric standardized drought indicators. Advances in Water Resources, 76, 140–145. doi:10.1016/j.advwatres.2014.11.012.

[41] Elbeltagi, A., Kumar, M., Kushwaha, N. L., Pande, C. B., Ditthakit, P., Vishwakarma, D. K., & Subeesh, A. (2023). Drought indicator analysis and forecasting using data driven models: case study in Jaisalmer, India. Stochastic Environmental Research and Risk Assessment, 37(1), 113–131. doi:10.1007/s00477-022-02277-0.

[42] Luo, B., Liu, X., Zhang, F., & Guo, P. (2021). Optimal management of cultivated land coupling remote sensing-based expected irrigation water forecasting. Journal of Cleaner Production, 308, 127370. doi:10.1016/j.jclepro.2021.127370.

[43] Lotfirad, M., Esmaeili-Gisavandani, H., & Adib, A. (2022). Drought monitoring and prediction using SPI, SPEI, and random forest model in various climates of Iran. Journal of Water and Climate Change, 13(2), 383–406. doi:10.2166/wcc.2021.287.

[44] Ali, M., Deo, R. C., Downs, N. J., & Maraseni, T. (2018). Multi-stage committee based extreme learning machine model incorporating the influence of climate parameters and seasonality on drought forecasting. Computers and Electronics in Agriculture, 152, 149–165. doi:10.1016/j.compag.2018.07.013.

[45] Patil, R., Polisgowdar, B. S., Rathod, S., Bandumula, N., Mustac, I., Srinivasa Reddy, G. V., Wali, V., Satishkumar, U., Rao, S., Kumar, A., & Ondrasek, G. (2023). Spatiotemporal Characterization of Drought Magnitude, Severity, and Return Period at Various Time Scales in the Hyderabad Karnataka Region of India. Water (Switzerland), 15(13), 2483. doi:10.3390/w15132483.

[46] Sobhani, B., & Zengir, V. S. (2020). Modeling, monitoring and forecasting of drought in south and southwestern Iran, Iran. Modeling Earth Systems and Environment, 6(1), 63–71. doi:10.1007/s40808-019-00655-2.

[47] Vicente-Serrano, S. M., Beguería, S., & López-Moreno, J. I. (2010). A multiscalar drought index sensitive to global warming: The standardized precipitation evapotranspiration index. Journal of Climate, 23(7), 1696–1718. doi:10.1175/2009JCLI2909.1.

[48] Statistical Centre of Iran. (2019). The concise report of the nationwide income-espense census of Iranian urban and rural households. Statistical Centre of Iran, Tehran, Iran. Available online: https://www.amar.org.ir/Portals/0/News/1398/ch-hvd97.pdf (accessed on May 2023).

[49] SCI. (2023). Statistical Centre of Iran, Tehran, Iran. Available online: https://www.amar.org.ir/english (accessed on May 2023).

[50] Karimi, Z. (2018). Public Works Programs as a Strong Means for Land and Water Conservation in Iran. Full Employment and Social Justice, 109–138. doi:10.1007/978-3-319-66376-0_5.

[51] Mesgaran, M. B., Madani, K., Hashemi, H., & Azadi, P. (2017). Iran's Land Suitability for Agriculture. Scientific Reports, 7(1), 7670. doi:10.1038/s41598-017-08066-y.

[52] Habibi, F., Rahmati, M., & Karimi, A. (2018). Contribution of tourism to economic growth in Iran's Provinces: GDM approach. Future Business Journal, 4(2), 261–271. doi:10.1016/j.fbj.2018.09.001.

[53] Nouri-Khajehbolagh, R., Khaledian, M., & Kavoosi-Kalashami, M. (2020). Comparison of water productivity indicators for major crops in Ardabil Plain. Iranian Journal of Irrigation & Drainage, 14(3), 894-904.

[54] Legates, D. R., & Willmott, C. J. (1990). Mean seasonal and spatial variability in gauge ‐ corrected, global precipitation. International Journal of Climatology, 10(2), 111-127. Portico. doi:10.1002/joc.3370100202.

[55] Sevruk, B., Ondrás, M., & Chvíla, B. (2009). The WMO precipitation measurement intercomparisons. Atmospheric Research, 92(3), 376–380. doi:10.1016/j.atmosres.2009.01.016.

[56] Saghafian, B., Tajrishy, M., Shahraini, H. T., & Jalali, N. (2003). Modeling spatial variability of daily rainfall in southwest Iran. Scientia Iranica, 10(2), 164 – 174).

[57] Doulabian, S., Golian, S., Toosi, A. S., & Murphy, C. (2021). Evaluating the effects of climate change on precipitation and temperature for iran using rcp scenarios. Journal of Water and Climate Change, 12(1), 166–184. doi:10.2166/wcc.2020.114.

[58] Gunathilake, M. B., Karunanayake, C., Gunathilake, A. S., Marasingha, N., Samarasinghe, J. T., Bandara, I. M., & Rathnayake, U. (2021). Hydrological Models and Artificial Neural Networks (ANNs) to Simulate Streamflow in a Tropical Catchment of Sri Lanka. Applied Computational Intelligence and Soft Computing, 2021, 1–9. doi:10.1155/2021/6683389.

[59] Javan, K., Lialestani, M. R. F. H., & Nejadhossein, M. (2015). A comparison of ANN and HSPF models for runoff simulation in Gharehsoo River watershed, Iran. Modeling Earth Systems and Environment, 1(4). doi:10.1007/s40808-015-0042-1.

[60] Molajou, A., Nourani, V., Afshar, A., Khosravi, M., & Brysiewicz, A. (2021). Optimal Design and Feature Selection by Genetic Algorithm for Emotional Artificial Neural Network (EANN) in Rainfall-Runoff Modeling. Water Resources Management, 35(8), 2369–2384. doi:10.1007/s11269-021-02818-2.

[61] Govindaraju, R. S. (2000). Artificial neural networks in hydrology. I: Preliminary concepts. Journal of Hydrologic Engineering, 5(2), 115-123. doi:10.1061/(asce)1084-0699(2000)5:2(115).

[62] Ouma, Y. O., Cheruyot, R., & Wachera, A. N. (2022). Rainfall and runoff time-series trend analysis using LSTM recurrent neural network and wavelet neural network with satellite-based meteorological data: case study of Nzoia hydrologic basin. Complex & Intelligent Systems, 8(1), 213–236. doi:10.1007/s40747-021-00365-2.

[63] Yu, N., & Haskins, T. (2021). Bagging machine learning algorithms: A generic computing framework based on machine-learning methods for regional rainfall forecasting in upstate New York. Informatics, 8(3), 47. doi:10.3390/informatics8030047.

[64] di Piazza, A., Conti, F. Lo, Noto, L. V., Viola, F., & La Loggia, G. (2011). Comparative analysis of different techniques for spatial interpolation of rainfall data to create a serially complete monthly time series of precipitation for Sicily, Italy. International Journal of Applied Earth Observation and Geoinformation, 13(3), 396–408. doi:10.1016/j.jag.2011.01.005.

[65] Tsesmelis, D. E., Leveidioti, I., Karavitis, C. A., Kalogeropoulos, K., Vasilakou, C. G., Tsatsaris, A., & Zervas, E. (2023). Spatiotemporal Application of the Standardized Precipitation Index (SPI) in the Eastern Mediterranean. Climate, 11(5), 95. doi:10.3390/cli11050095.

[66] Irawan, A. N. R., Komori, D., & Hendrawan, V. S. A. (2023). Correlation analysis of agricultural drought risk on wet farming crop and meteorological drought index in the tropical-humid region. Theoretical and Applied Climatology, 153(1–2), 227–240. doi:10.1007/s00704-023-04461-w.

[67] Moccia, B., Mineo, C., Ridolfi, E., Russo, F., & Napolitano, F. (2022). SPI-Based Drought Classification in Italy: Influence of Different Probability Distribution Functions. Water (Switzerland), 14(22), 3668. doi:10.3390/w14223668.

[68] McKee, T. B., Doesken, N. J., & Kleist, J. (1993). The relationship of drought frequency and duration to time scales. Proceedings of the 8th Conference on Applied Climatology, 17-22 January, 1993, Anaheim, United States.

[69] Park, C., Min, S. K., Lee, D., Cha, D. H., Suh, M. S., Kang, H. S., Hong, S. Y., Lee, D. K., Baek, H. J., Boo, K. O., & Kwon, W. T. (2016). Evaluation of multiple regional climate models for summer climate extremes over East Asia. Climate Dynamics, 46(7–8), 2469–2486. doi:10.1007/s00382-015-2713-z.

[70] Yang, Y., Bai, L., Wang, B., Wu, J., & Fu, S. (2019). Reliability of the global climate models during 1961–1999 in arid and semiarid regions of China. Science of the Total Environment, 667, 271–286. doi:10.1016/j.scitotenv.2019.02.188.

[71] Leirvik, T., & Yuan, M. (2021). A Machine Learning Technique for Spatial Interpolation of Solar Radiation Observations. Earth and Space Science, 8(4), 2020 001527. doi:10.1029/2020EA001527.

[72] Ciscar, J. C., Rising, J., Kopp, R. E., & Feyen, L. (2019). Assessing future climate change impacts in the EU and the USA: Insights and lessons from two continental-scale projects. Environmental Research Letters, 14(8), 84010. doi:10.1088/1748-9326/ab281e.

[73] He, Q., Wang, M., Liu, K., Li, K., & Jiang, Z. (2022). GPRChinaTemp1km: A high-resolution monthly air temperature data set for China (1951-2020) based on machine learning. Earth System Science Data, 14(7), 3273–3292. doi:10.5194/essd-14-3273-2022.

[74] Amininia, K., Abad, B., Safarianzengir, V., GhaffariGilandeh, A., & Sobhani, B. (2020). Investigation and analysis of climate comfort on people health tourism in Ardabil province, Iran. Air Quality, Atmosphere & Health, 13(11), 1293–1303. doi:10.1007/s11869-020-00883-x.